Bioorganic & Medicinal Chemistry Letters 21 (2011) 5480–5486

Contents lists available at ScienceDirect

Bioorganic & Medicinal Chemistry Letters

journal homepage: www.elsevier.com/locate/bmcl

Structure-based optimization of potent 4- and 6-azaindole-3-carboxamides as renin inhibitors

Bodo Scheiper [a], Hans Matter [a,*], Henning Steinhagen [a,†], Zsolt Böcskei [b], Valérie Fleury [c], Gary McCort [c]

[a] Sanofi-Aventis, Deutschland GmbH, Chemical and Analytical Sciences, Building G878, D-65926 Frankfurt, Germany
[b] Sanofi-Aventis, Chemical and Analytical Sciences, 16 Rue d'Ankara, F-67080 Strasbourg, France
[c] Sanofi-Aventis, Cardiovascular Department, 1 Avenue Pierre Brossolette, F-91385 Chilly-Mazarin, France

ARTICLE INFO

Article history:
Received 9 May 2011
Revised 24 June 2011
Accepted 26 June 2011
Available online 6 July 2011

Keywords:
Renin
Azaindole
Structure-based-design
Aspartyl-protease

ABSTRACT

The control of hypertension and associated cardiovascular risk factors is possible by selective inhibition of the aspartyl protease renin due to its unique position in the renin-angiotensin system. Starting from a previously disclosed series of potent and nonchiral indole-3-carboxamides, we further explored this motif by structure-based drug design guided by X-ray crystallography in combination with efficient parallel synthesis. This resulted in the discovery of 4- or 6-azaindole derivatives with remarkable potency for renin inhibition. The best compound from these series showed an IC_{50} value of 1.3 nM.

Hypertension is one of the primary risk factors for cardiovascular diseases which are one of the primary causes of mortality today in the Western world.[1] In this situation, a lower blood-pressure can considerably reduce the risk of myocardial infarction, stroke, heart failure and end-stage kidney disease.[2] However, as several patients do not fully respond to current blood-pressure lowering medications, there is still a medical need for further developing well-tolerated medicines to control hypertension.

The renin-angiotensin system (RAS) is an endocrine system, which is involved in the regulation of blood pressure and fluid electrolytes. It is activated by various signals in normotensive humans including the reduction of blood pressure, decrease in circulating blood volume and plasma-sodium concentration.[3] Following RAS activation, the aspartyl protease renin with 340 amino acids is released from the kidney; it cleaves the peptide angiotensinogen at its Leu^{10}–Val^{11} bond to produce the decapeptide angiotensin I, which is converted to angiotensin II by the angiotensin converting enzyme (ACE). Angiotensin II then addresses two main receptor subtypes AT_1 and AT_2 for its physiological effect. Since the hydrolysis by renin is the rate-limiting step in this cascade and angiotensinogen is the only known substrate for renin, inhibition of this step is perceived a very effective antihypertensive strategy.[4]

Consequently, substantial efforts during the last years were directed towards identification of novel series of renin inhibitors with improved bioavailability and pharmacological properties for use in clinical settings. Aliskiren (SPP100) is an orally active renin inhibitor with four chiral centers (Fig. 1). It is today the only direct renin inhibitor, which has reached the market.[5]

In a recent publication[6] we reported the discovery of a novel class of nonchiral indole-3-carboxamides as renin inhibitors. The incorporation of substituted phenoxy- or benzyl groups into compounds **1a** and **1b** (Fig. 1) combined with adequate decoration at the indole core led to a significant improvement of activity. The best compound **1c** (Fig. 1) shows an IC_{50} value of 0.002 μM and is very selective against other proteases.

In this publication we describe the discovery, structure–activity-relationship and optimization of 4- and 6-azaindole-3-carboxamides as renin inhibitors[7], which are derived by structure-based design guided by X-ray crystallography in combination with efficient parallel synthesis. Further investigations towards other scaffolds will be discussed in an accompanying publication.

The X-ray crystal structure of the indole lead structure **1c** in complex with renin (PDB 3OOT, Fig. 2) at 2.5 Å resolution[6] reveals a "closed-flap" conformation, as also observed for Aliskiren (PDB 2V0Z).[8] This binding mode was used as template for structure-based design. The piperazine moiety is engaged in ionic hydrogen-bond interactions to both aspartates Asp^{32} and Asp^{215}, while the neighboring carboxamide oxygen interacts with Thr^{77}–OγH. Both phenyl rings are involved in lipophilic interactions to the renin S1 and S3 pockets. The 2-methyl-3-fluoro-benzyl group

* Corresponding author. Tel.: +49 69 305 84329.
E-mail address: Hans.Matter@sanofi-aventis.com (H. Matter).
† Present address: Grünenthal Pharma GmbH, Global Drug Discovery, Zieglerstr. 6, 52099 Aachen, Germany.

0960-894X/$ - see front matter © 2011 Published by Elsevier Ltd.
doi:10.1016/j.bmcl.2011.06.114

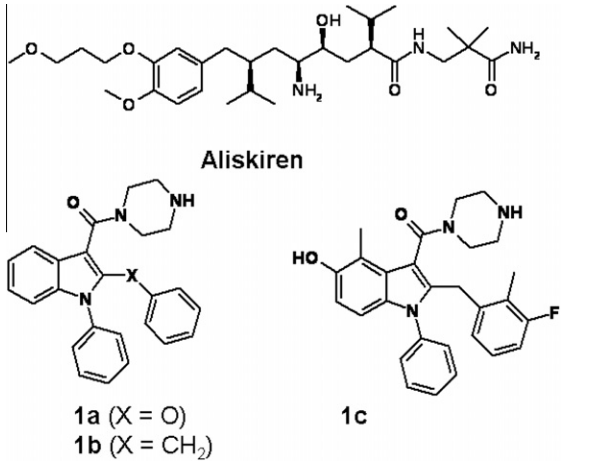

Figure 1. Chemical structures of renin inhibitors: Aliskiren, 3-indole-carboxamides **1a** (IC_{50} 0.420 μM), **1b** (0.091 μM) and lead structure **1c** (0.002 μM).

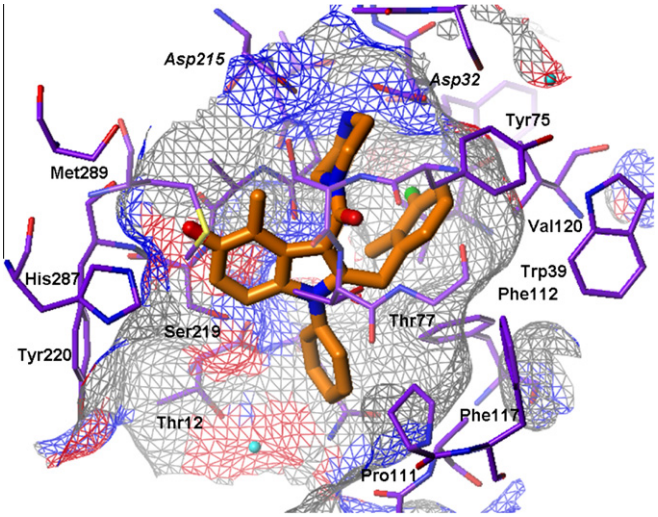

Figure 2. X-ray crystal structure of indole **1c** (PDB 3OOT, orange carbons, 2.5 Å resolution) in complex with human renin. The protein binding site is indicated using a MOLCAD[11] hydrogen bonding surface. Crystallographic water is indicated by cyan spheres.

optimally fills the S1 pocket with fluorine in a lipophilic subpocket. The close distance between fluorine and the Asp^{32} carboxylate also suggests an orthogonal multipolar interaction.[9,10] The 2-methyl group is pointing towards a lipophilic region consisting of Gly^{217}-Cα, Val^{30}Cγ and the Phe^{117} aromatic ring. Furthermore a favorable edge-to-face type CH-π interaction between the S1 benzyl ring and Tyr^{75} is present (C-centroid distance = 3.53 Å). Substituents of the indole moiety also favorably contribute to affinity, in particular its 5-OH group, which is involved in a hydrogen-bond interaction to the His^{287} imidazole, while the 4-methyl substituent contacts the side chain atoms of Thr^{77}Cγ.

The positive effect of polar substitutions at the indole core prompted us to explore other isosteric ring systems. Hence, after analysis of renin-indole X-ray structures[6], we set out to systematically explore azaindole derivatives with respect to renin activity and favorable physicochemical properties. The introduction of nitrogen atoms into positions 4 or 6 of the indole system results in scaffolds with similar vectors orient side chains towards their site of interaction. However, this modification affects charge distribution and thus polarity of neighboring aromatic C–H fragments,

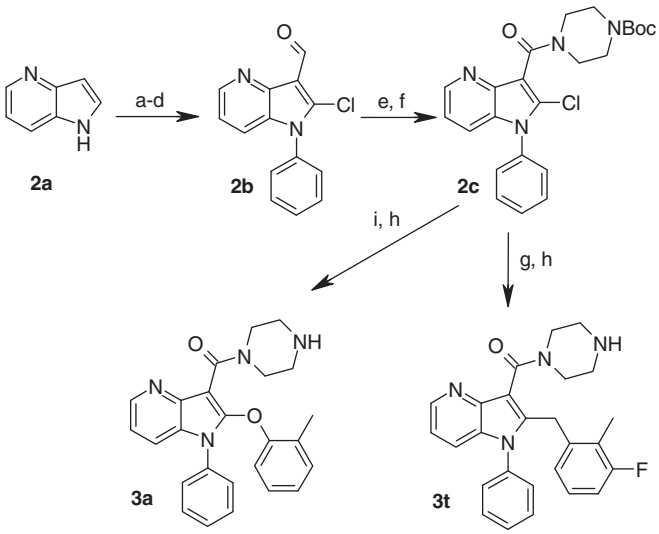

Scheme 1. Synthesis of compounds **3a** and **3t**. Reagents: (a) CuI, 8-hydroxyquinoline, phenyliodide, K_2CO_3, DMSO, 130 °C, 28%; (b) Br_2, *t*-BuOH, H_2O, rt; (c) Pd/C, H_2, EtOH, rt, 99% over both steps; (d) (i) $POCl_3$, DMF, DCM, pyridine, 0 °C → rt, (ii) $POCl_3$, DCM, 100 °C, 64%; (e) $NaClO_2$, NaH_2PO_4, *t*-BuOH, rt, 88%; (f) *N*-Boc-piperazine, TOTU, NMM, DMF, rt, 52%; (g) (i) 3-Fluoro-2-methyl-benzylbromide, Zn, THF, 0 °C, (ii) 9-MeO-9-BBN, −78 °C → rt, (iii) $Pd(OAc)_2$, *S*-Phos, DMF, 100 °C, 73%; (h) TFA, DCM, rt, quant.; (i) 2-Methylphenol, NaH, NMP, rt → 140 °C, microwave, 58%.

allowing for favorable polar interactions to the protein binding site. In particular, we were aiming to interact with the imidazole side chain of His^{287} either directly or via a structurally conserved water molecule, which is present in related X-ray structures. This water is linking the His^{287} imidazole to the backbone amide nitrogen of Tyr^{220}. Furthermore this substitution will also modulate physicochemical properties like lipophilicity and basicity of the lead series. Here, the computed log *D* for indole derivatives (**1a**: 1.8, **1b**: 2.4) is significantly decreased for 4-azaindoles (S1-phenoxy: 0.8, S1-benzyl: 1.4) and 6-azaindoles (S1-phenoxy: 0.7, S1-benzyl: 1.3), respectively.[12]

The synthetic pathway for the preparation of compound series **3** to **7** is outlined in Scheme 1 representatively for examples **3a** and **3t** from Table 1. 4-Azaindole **2a** was arylated under copper catalysis[13], then oxidized with bromine and subsequently reduced according to the procedure of Robinson.[14] Vilsmeier–Haack formylation with concomitant chlorination then yielded aldehyde **2b**. Subsequent oxidation to the acid and coupling with *N*-Boc-piperazine provided the key intermediate **2c**. This chloride **2c** was then either coupled in a palladium-mediated reaction followed by deprotection to the corresponding benzyl derivative **3t** or submitted to nucleophilic substitution to provide the arylether derivative **3a**. The synthesis of all other derivatives **3** to **7** was carried out accordingly to this scheme. All substituted piperazine derivatives for compound series **4** were commercially available; *N*-Boc was also employed as protecting group.

Table 1 summarizes a representative collection of 4-azaindole derivatives **3a–3t** with experimental IC_{50} values [μM]. To calculate IC_{50} values, the activity of an inhibitor was evaluated in a 10 point concentration range in intraplate duplicates. Two to four independent experiments were performed. The IC_{50} is expressed as geometric mean ± standard deviation (SD), which in general was low for this assay.[6,7,15]

These variations within the S1 pocket (Table 1) resulted in improved affinity compared to **1a** and **1b**.[6] Adding an ortho-methyl to the phenoxy-ring resulted in compound **3a** with an IC_{50} value of 0.25 μM. However, comparing **3a** with its identical substituent attached to the indole shows a 12-fold better activity for this indole derivative (see **2e** in Ref. 6 with 0.021 μM). Adding another methyl

Table 1
In vitro activity for compounds **3a**–**3t**[a]

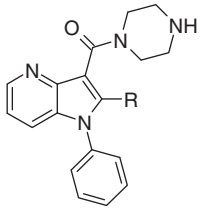

Compds	R	Renin IC_{50} [μM][a]
3a	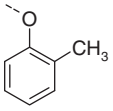	0.25
3b	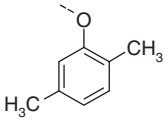	0.692
3c	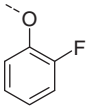	0.513
3d	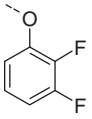	0.310
3e	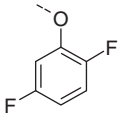	0.202
3f	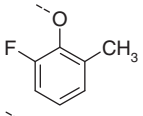	0.074
3g	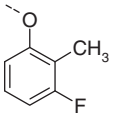	0.057
3h	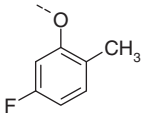	0.024
3i	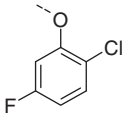	0.055
3j	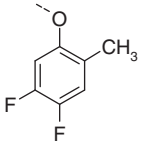	0.322
3k	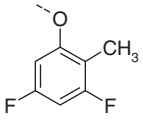	0.107
3l	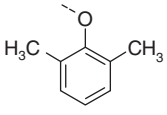	0.014
3m		0.0013

Table 1 (*continued*)

Compds	R	Renin IC_{50} [μM][a]
	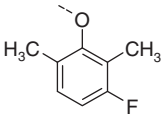	
3n	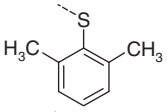	0.061
3o	Benzyl	0.939
3p	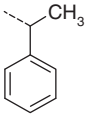	1.000
3q	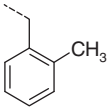	0.12
3r	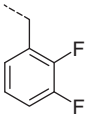	1.460
3s	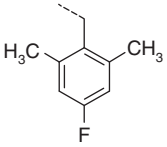	0.246
3t	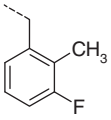	0.012

[a] IC_{50} data were obtained as described in the text and in Ref. 7

group in meta-position (**3b**, 0.692 μM) or replacing the ortho-methyl by fluorine (**3c**, 0.513 μM) does not further improve renin affinity in the 4-azaindole series.

Systematic variations then led us to incorporate the most active substituents from the indole series in addition to further building blocks for this S1 pocket. This optimization resulted first in the arylether **3h** (0.024 μM) with a 2-methyl-5-fluoro-phenoxy-substitution. However, again the corresponding indole analog was fivefold more active (see **2j** in Ref. 6 with 0.005 μM). Shifting the fluorine substituent to position 3 or 6 at the S1-directed phenoxy-derivative in the 4-azaindole series resulted in compounds **3g** (0.057 μM) and **3f** (0.074 μM), which are again about a factor of 5 less active than the corresponding indole derivatives. The incorporation of a 2,6-dimethylphenoxy-substituent then resulted in compound **3l** with an IC_{50} value of 0.014 μM. This improved affinity was quite remarkable in comparison to the 2-fluoro-6-methylphenylether **3f** with an IC_{50} value of only 0.074 μM and to the indole analog with an IC_{50} value of 0.064 μM (see **2i** in Ref. 6), respectively.

The subsequent analysis of the structure–activity relationship for this series in combination with inspection of the X-ray structure information then led us to combine the substitution motifs from **3h** and **3l**, resulting in the very potent compound **3m** with a 2,6-dimethyl-3-fluoro-phenoxy-substituent directed towards the renin S1 pocket and an IC_{50} value of 0.0013 μM.

The derivatives **3o**–**3t** then were synthesized to explore benzyl groups oriented towards the S1 pocket. Most derivatives are again less active in the 4-azaindole series in comparison to the indole

Table 2
In vitro activity for compounds **4a**–**4n**[a]

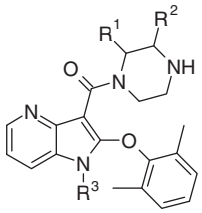


R³ = A


R³ = B

Compds	R^1	R^2	R^3	Renin IC_{50} [μM][a]
4a	H	H	A	0.004
4b	H	*S*-CH_3	A	0.080
4c	H	*S*-CH_3	B	0.060
4d	H	*R*-CH_2OH	A	0.390
4e	H	*R*-CH_2OH	B	0.143
4f	H	*R*-CH_2OCH_3	A	0.694
4g	H	*R*-CH_2OCH_3	B	0.290
4h	H	*S*-CH_2CH_3	B	0.455
4i	H	*S*-Pr	B	1.180
4j	H	*S*-^{i}Pr	B	2.710
4k	H	*rac*-Bu	B	0.285
4l	H	*rac*-$CH_2CO_2CH_3$	B	0.057
4m	H	*rac*-$CH_2CONHCH_3$	B	0.070
4n	*S*-Benzyl	H	B	0.152

[a] IC_{50} data were obtained as described in the text and in Ref. 7

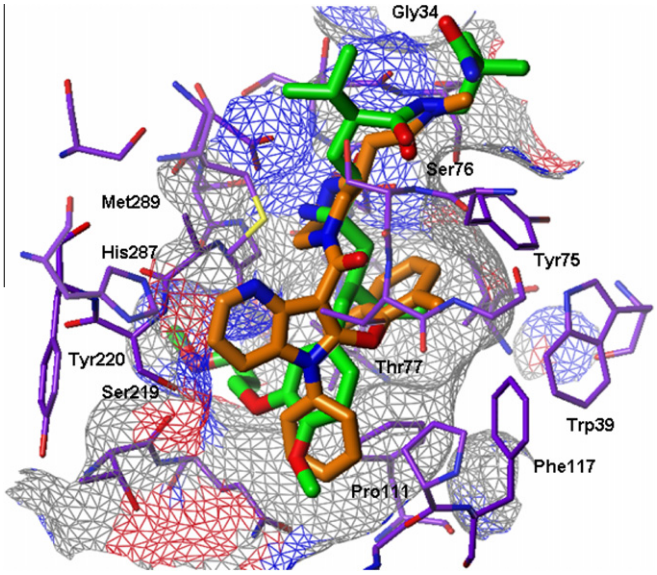

Figure 3. Binding pose of compound **4m** (orange carbons) from docking into the renin binding site from the X-ray crystal structure of **1c**. In addition the X-ray structure of Aliskiren (PDB 2V0Z, resolution 2.2 Å) is displayed (green carbons).

series.[6] The unsubstituted benzyl-derivative is about 10-fold less active in the 4-azaindole series (**3o**, 0.939 μM). While methylation of the benzyl–CH_2 linker does not improve activity (**3p**, 1.0 μM), adding a methyl-group in ortho-position of the benzyl ring resulted in **3q** (0.12 μM), thus being more active as the phenylether-derivative **3a** with 0.25 μM.

Further analysis of related substituents then revealed that structure–activity trends are not strictly linear in phenoxy- or benzyl-4-azaindole series, as it was also observed for the indole SAR. This can be illustrated by comparing **3a**/**3q** (0.25/0.12 μM) with ortho-methyl substitutions with the derivatives **3d**/**3r** (0.31/1.46 μM) with 2,3-difluoro-substituents and an inverse activity trend. The corresponding benzyl-derivative **3t** with ortho-methyl and meta-F substitution was identified as most active derivative with an IC_{50} value 0.012 μM. To our surprise, its activity was almost similar for the corresponding indole derivative (see example **2n** in Ref. 6 with 0.009 μM). From docking[16–18] into the X-ray structure of **1c**, a similar binding mode of **3t** with its substituted benzyl group oriented accordingly is postulated. The 4-azaindole-nitrogen points towards a more lipophilic area formed by Thr^{77}–Cγ and Ala^{218}–Cβ atoms.

The nonrelated SAR between 4-azaindoles and indoles prompted for further evaluation of this scaffold by replacing the 4-azaindole-N^1 group and adding substituents to the piperazine ring. A representative subset of molecules is summarized in Table 2. The replacement of the N^1 phenyl-group against the larger, lipophilic cyclohexyl-substituent (R^3 = A in Table 2) resulted in threefold improved affinity when comparing the N^1 cyclohexyl-derivative **4a** (0.004 μM) to the corresponding N^1-phenyl derivative **3l** (0.014 μM). Interestingly, the comparison of entries **4b** to **4c** reveals a reversed trend for these analogs with an additionally methylated piperazine group. Here the cyclohexyl-derivative **4b** is slightly less active with an IC_{50} value of 0.080 μM compared to the phenyl derivative **4c** with an IC_{50} value of 0.060 μM. The same trend with slightly reduced renin affinity for the N^1-cyclohexyl-derivative is observed for entries **4d** (0.390 μM) versus **4e** (0.143 μM) and **4f** (0.694 μM) versus **4g** (0.290 μM), which is consistent with observations for the indole scaffold. These findings still underscore the hydrophobic nature of this interaction with either a phenyl- or cyclohexyl-group in the renin S3-subpocket. However, this analysis also reveals different SAR trends for unsubstituted versus substituted piperazines, which might be due to differing orientations of the S3 substituent, being more compatible with the smaller phenyl-group in S1.

Chiral substitutions at the piperazine were introduced after comparing Aliskiren (PDB 2V0Z)[8] to the indole binding pose. The bond vector connecting the aminoethanol to its isobutyl-carboxyamide in the S1′-pocket is aligned with the vector C^2–$H^{pro\text{-}S}$ next to the secondary amine function (R^2 in Table 2).

Molecular modeling suggested that lipophilic replacements at the piperazine could be also directed towards this S1′ subpocket area, thus also impacting activity. While the lipophilic *S*-methyl substituent resulted in the potent derivative **4c** (0.060 μM), activity was lower in general, if the chain length of the substituent was increased (e.g., **4h** with ethyl and 0.455 μM) or polarity introduced (e.g., **4e** with *R*-hydroxymethyl and 0.143 μM; please note related vectors despite different chirality nomenclature). Adding an *S*-benzyl substituent to the piperazine ring next to its carboxamide linkage is also tolerated, but does apparently not improve affinity substantial as exemplified by **4n** with an IC_{50} value of 0.152 μM (substituent at R^1 in Table 2).

However, introducing a hydrogen-bonding acceptor into this S1′ directed side chain now results in increased activity, as exemplified by entries **4l** and **4m** in Table 2. Both molecules contain a carbonyl group in this side chain, which is postulated to be involved in a hydrogen-bonding interaction to Ser^{76}–NH from docking (distance O···Ser^{76}–NH 2.29 Å). The neighboring amide group in **4m** does only slightly improve binding affinity to result in an IC_{50} value of 0.070 μM, despite its potential involvement in an additional hydrogen bond to Gly^{34}–C=O, as postulated from docking (distance NH···Gly^{34}–C=O 2.03 Å) and its analogy to the Aliskiren binding mode. This binding mode of **4m** from docking into renin is displayed in Figure 3 in comparison to Aliskiren (green carbons). Surprisingly the replacement of the **4m** carboxyamide by an ester in entry **4l** further improves affinity to result in an IC_{50} value of 0.057 μM, thus underscoring that the additional hydrogen-bonding interaction in **4m** is not essential for affinity gain.

Next we set out to decorate the 4-azaindole core with substituents in order to gain further activity in this series. In the indole series, several polar groups like hydroxyl in this area in the protein

pocket display a slightly positive effect on affinity, in particular the 5-OH substitution, for example, exemplified in derivative **1c** (IC_{50} 0.002 μM) with the OH group engaged in a hydrogen-bond interaction to the His[287] side chain. Representative results for 4-azaindoles with three different phenoxy- and benzyl substituents at position R^2 are summarized in Table 3. When comparing these derivatives to the reference 4-azaindole **3h** (IC_{50} 0.024 μM, R^2 = A), none of the groups in 5-position exhibit a positive effect on renin activity. While in agreement to the indole series a 5-methoxy group reduces affinity (**5a** 6.63 μM, **5h** 0.59 μM), the same effect is seen when adding a polar 5-OH group (**5b** >5.0 μM, **5i** 1.60 μM), thereby significantly conflicting with the SAR for the related indole series. In particular for the 5-hydroxy-4-azaindoles, our closer analysis by computational estimation of tautomers ratios[19] suggests that the pyridone as alternative tautomer is exclusively present in solution or in the protein binding site. Hence, this tautomer exhibits apparently a carbonyl group in position 5, which cannot favorably interact via a hydrogen-bond to His[287].

Structure-based design based on the X-ray structure of **1c** further suggested the possibility to add lipophilic substituents to the azaindole 6-position. Some lipophilic substitutions in 6-position at the 4-azaindole core combined with a substituted benzyl group in S1 are better tolerated, as exemplified for compound **5e** with an IC_{50} value of 0.08 μM. A small lipophilic 6-methyl substituent even results in similar or slightly increased affinity in compounds **5c** (0.014 μM) and **5g** (0.009 μM) in comparison to the references **3h** (0.024 μM) for the phenylether subseries and **3t** with 0.012 μM for the benzyl subseries. Thus, lipophilicity in this area has a slightly positive effect on activity. Remarkably, the introduction of a 6-OH group without any possibility for tautomerization resulted in the active compound **5d** (0.003 μM) in comparison to **3l** (0.014 μM). Here we postulate a favorable hydrogen-bond interaction to His[287], which is geometrically possible also from the 6-position of this scaffold.

Next we explored variations around the 6-azaindole core structure (Table 4). While entry **6a** with an IC_{50} value of 0.494 μM is less active as its 4-azaindole analog **3a** (IC_{50} 0.25 μM), substitutions at the phenylether moiety in S1 significantly improve affinity. This is shown by entry **6b** with an additional *meta*-fluorine substituent (0.027 μM). Here the corresponding 4-azaindole is almost equally potent (**3h**, 0.024 μM). Further decorations at the phenylether following the SAR of the 4-azaindoles further improved affinity, finally resulting at the potent compound **6d** with an IC_{50} value of 0.002 μM. Here the corresponding 4-azaindole **3m** is only slightly more active (0.0013 μM).

Again also the substitution of adequately decorated benzyl-groups led to highly potent 6-azaindoles. While the original benzyl-substituted derivative **6e** shows an activity of 0.761 μM (cf. 4-azaindole **3o**, IC_{50} 0.939 μM), the addition of the consistently best substituent in the benzyl subseries with an *ortho*-methyl and *meta*-fluoro-substitution improved activity to result at compound **6f** with 0.014 μM. Again, the corresponding 4-azaindole **3t** was equally active (0.012 μM).

Finally we introduced variations at the 6-azaindole core to further explore polar and hydrophobic interactions with the binding site to increase affinity. The resulting derivatives are summarized in Table 5. The addition of another small lipophilic methoxy substituent at position 5 (R^3 in Table 5) to compound **6f** of the 6-azaindole-benzyl-subseries resulted in entry **7a** with a significant loss of affinity (IC_{50} 0.850 μM), thus consistently showing that related substitutions in this position 5 of indoles and azaindoles have a less favorable effect to renin affinity. Hence, we then focused on variations of the 7-position in 6-azaindoles (R^2 in Table 5). Adding lipophilic substituents to the phenylether-derivative **6b** results in a decrease of affinity, as exemplified for entries **7b** with 7-Cl (0.320 μM) and **7c** with a 7-ethyl group (0.423 μM). However, the careful inspection of the renin-indole X-ray structures suggested that larger lipophilic substituents should be accommodated in the more open region of the renin binding site. This led to the synthesis of compound **7d** with a benzyl group in 7-position of the azaindole and an IC_{50} value of 0.003 μM, thus showing a ninefold improvement in binding affinity compared to **6b**. A similar positive effect was also observed for the benzyl series. Here a related

Table 3
In vitro activity for compounds **5a–5i**[a]

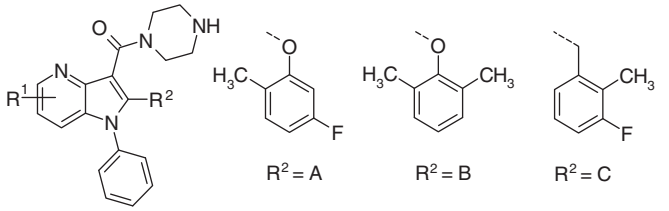

Compds	R^1	R^2	Renin IC_{50} [μM][a]
5a	5-OCH_3	A	6.630
5b	5-OH	A	>5.000
5c	6-CH_3	A	0.014
5d	6-OH	B	0.003
5e	6-OCH_2CH_3	B	0.08
5f	6-OCH_2CO_2H	B	0.11
5g	6-CH_3	C	0.009
5h	5-OCH_3	C	0.59
5i	5-OH	C	1.60

[a] IC_{50} data were obtained as described in the text and in Ref. 7

Table 4
In vitro activity for compounds **6a–6f**[a]

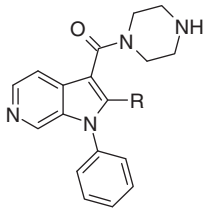

Compds	R	Renin IC_{50} [μM][a]
6a	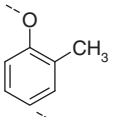	0.494
6b	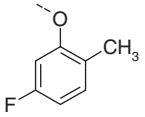	0.027
6c	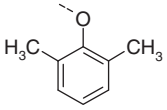	0.112
6d	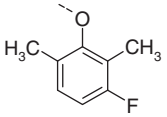	0.002
6e	Benzyl	0.761
6f	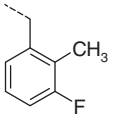	0.014

[a] IC_{50} data were obtained as described in the text and in Ref. 7

Table 5
In vitro activity for compounds **7a–7f**

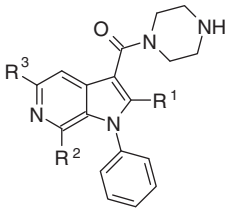

Compds	R^1	R^2	R^3	Renin IC_{50} [μM][a]
7a	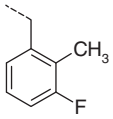	H	OCH_3	0.850
7b	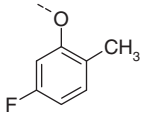	Cl	H	0.320
7c	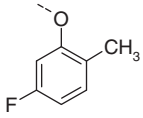	Et	H	0.423
7d	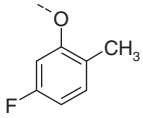	Bn	H	0.003
7e	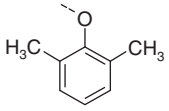	Cl	H	0.517
7f	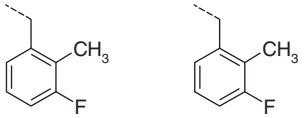		H	0.005

[a] IC_{50} data were obtained as described in the text and in Ref. 7

substitution in position 7 at the 6-azaindole scaffold with a large lipophilic benzyl derivative also resulted in an affinity enhancement, when comparing entry **7f** with an IC_{50} value of 0.005 μM to **6f** (0.014 μM).

We then solved the X-ray structure of the potent 6-azaindole **7d** in complex with human renin at a resolution of 2.1 Å (Fig. 4), thereby validating our hypothesis about favorable protein–ligand interactions.[20] In general, the binding mode is conserved when comparing to the structure of **1c** with essential interactions maintained, namely the piperazine-aspartate ionic interaction, the Thr^{77}–Oγ H hydrogen bond, the lipophilic interactions of both phenyl rings in S1 and S3, and the CH–π interaction in S1. Other interactions also contribute to the high affinity binding of **7d**.

One of the significant differences between **1c** and **7d** is the substituent directed towards S1, which is a phenylether-derivative for **7d**, but a benzyl-derivative for **1c**. Interestingly, for S1-directed phenylethers the 2-methyl-5-fluoro substitution leads to consistently higher affinity (**3h**, 0.024 μM vs **3g**, 0.057 μM), while benzyl-groups using 2-methyl-3-fluoro substituents are preferred for indoles[6] and 4-or 6 azaindoles. In accord with **1c**, the 5-fluorine substituent in **7d** is situated in the lipophilic subpocket close to the Asp^{32} carboxylate, again with a topology suggesting an additional orthogonal multipolar interaction.[9,10] In contrast to the orientation of the 2-methyl-3-fluoro-benzyl group in **1c**, the 2-methyl group in entry **7d** points towards the opposite site of the S1 pocket, thus contacting the lipophilic side chains of residues

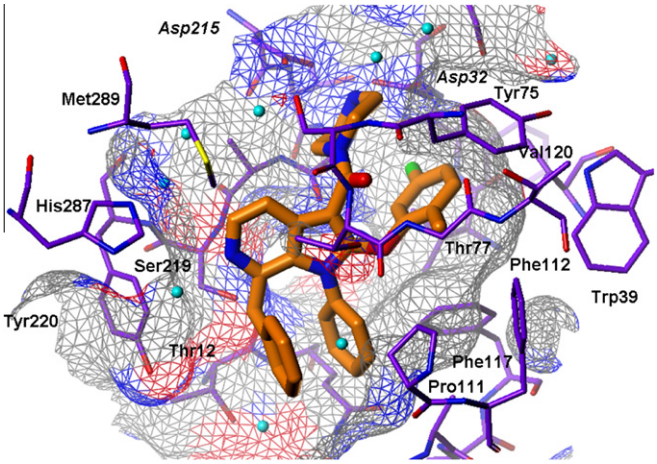

Figure 4. X-ray crystal structure of 6-azaindole **7d** (orange carbons, 2.1 Å resolution) in complex with human renin. Crystallographic water is indicated by cyan spheres.

Pro^{111} (distance: 4.54 Å) and Phe^{112} (distance: 3.84 Å). The dihedral angles of the phenoxy- or benzyl substituents directed towards S1 are only slightly different (C^2_{Indole}-X-C^1_{Phenyl}-C^2_{Phenyl} with X = O 124.3° and X = C 116.2°).

The 7-benzyl substitution at the 6-azaindole also favorably contributes to affinity. This group is oriented towards the more open area of the pocket towards the lipophilic side chains of Pro^{111} and Leu^{114}, involved in an intramolecular π–π interaction[21] to the azaindole-N^1-phenyl ring, which stabilizes its conformation (centroid distance 3.83 Å). There is an indirect interaction from the azaindole 6-nitrogen to the His^{287} imidazole side chain via a water molecule (distance azaindole-N^6···water: 3.03 Å; water··· imidazole–N: 2.93 Å).

This imidazole side chain is contacting a second water via its other nitrogen (distance 3.03 Å), which itself interacts with the backbone amide nitrogen of Tyr^{220}. This combination of favorable interactions accounts for the increased affinity of **7d** in comparison to **6b**.

Selected compounds were profiled using IC_{50} values in human or mouse plasma plus Caco-2 and physicochemical data[22] (Table 6). The best compounds display IC_{50} values between 1.3 and 14 nM without significant activity reduction in plasma. Furthermore, higher Caco-2 Papp values for **3m**, **6f**, and **7d** suggest potential for intestinal absorption. **3m** in particular is interesting for optimization based on its balance between lipophilicity, affinity and ligand efficiency.

In summary we have described the design and structure–activity relationship of a novel series of potent renin inhibitors based on 4- or 6-azaindole scaffolds. Both scaffolds were developed from a previous series of indole-3-carboxamides. Although general structure–activity trends were found to be correlated, there is no strict linearity upon transferring substituents. This prompted us to explore both novel scaffolds with a preferred set of building blocks directed to S1. Other parts of the scaffolds were decorated to arrive at high affinity and favorable physicochemical properties. In particular, the incorporation of substituted phenoxy- or benzyl S1 derivatives plus substitution at the azaindole core led to a significant improvement of affinity.

The availability of X-ray structures of renin-inhibitor complexes during our optimization allowed us to unveil the key determinants to affinity. Further details on the optimization of 5- and 7-azaindoles will be reported in an accompanying publication. In summary this collection of isosteric scaffolds constitutes a promising area for further structure-based design and facilitates adjustment of physicochemical properties.

Table 6
Further profiling of selected Renin inhibitors[a]

Cpds	Renin IC_{50} [μM]	Renin IC_{50} with human plasma [μM]	Renin IC_{50} with mouse plasma [μM]	Caco-2 Permeability Papp [$*10^{-7}$ cm/s]	Log *P* (MoKa)	pKa (basic, MoKa)	Log *D* (pH 7.4, MoKa)	Ligand efficiency	Lipophilic ligand efficiency
3l	0.014	0.030	0.015	2.8	2.1	8.1	1.3	0.33	5.75
3m	0.0013	nd	0.036	43	2.3	8.1	1.5	0.37	6.59
6f	0.014	0.025	0.026	12.7	2.5	8.1	1.7	0.33	5.35
7d	0.003	0.226	0.192	39	3.7	8.1	2.9	0.30	4.82

[a] Data were obtained as described in text and ref. 22. nd = not determined.

Acknowledgements

The authors would like to thank Sabrina Berger, Holger Gaul, Silvia Hein, Laetitia Martin, Andrea Müller, Mathilde Pierre, and Katja Wittmann for their technical assistance.

References and notes

1. Kearney, P. M.; Whelton, M.; Reynolds, K.; Muntner, P.; Whelton, P. K.; He, J. *Lancet* **2005**, *365*, 217.
2. (a) Amin Zaman, M.; Oparil, S.; Calhoun, D. A. *Nat. Rev. Drug Disc.* **2002**, *1*, 621; (b) Jensen, C.; Herold, P.; Brunner, H. R. *Nat. Rev. Drug Disc.* **2008**, *7*, 399.
3. MacGregor, G. A.; Markandu, N. D.; Roulston, J. E.; Jones, J. E.; Morton, J. J. *Nature* **1981**, *291*, 329.
4. Wood, J. M.; Stanton, J. L.; Hofbauer, K. G. *J. Enzyme Inhib. Med. Chem.* **1987**, *1*, 169.
5. (a) Göschke, R.; Stutz, S.; Rasetti, V.; Cohen, N.-C.; Rahuel, J.; Rigollier, P.; Baum, H.-P.; Forgiarini, P.; Schnell, C. R.; Wagner, T.; Grütter, M. G.; Fuhrer, W.; Schilling, W.; Cumin, F.; Wood, J. M.; Maibaum, J. *J. Med. Chem.* **2007**, *50*, 4818; (b) Maibaum, J.; Stutz, S.; Göschke, R.; Rigollier, P.; Yamaguchi, Y.; Cumin, F.; Rahuel, J.; Baum, H.-P.; Cohen, N.-C.; Schnell, C. R.; Fuhrer, W.; Grütter, M. G.; Schilling, W.; Wood, J. M. *J. Med. Chem.* **2007**, *50*, 4832.
6. Scheiper, B.; Matter, H.; Steinhagen, H.; Stilz, U.; Böcskei, Z.; Fleury, V.; McCort, G. *Bioorg. Med. Chem. Lett.* **2010**, *20*, 6268.
7. Steinhagen, H.; Scheiper, B.; Matter, H.; McCort, G. *PCT Int. Appl.* **2009**, WO 2009095162.
8. Rahuel, J.; Rasetti, V.; Maibaum, J.; Rüeger, H.; Göschke, R.; Cohen, N.-C.; Stutz, S.; Cumin, F.; Fuhrer, W.; Wood, J. M.; Grütter, M. G. *Chem. Biol.* **2000**, *7*, 493.
9. (a) Böhm, H.-J.; Banner, D.; Bendels, S.; Kansy, M.; Kuhn, B.; Müller, K.; Obst-Sander, U.; Stahl, M. *ChemBioChem* **2004**, *5*, 637; (b) Olsen, J. A.; Banner, D. W.; Seiler, P.; Obst-Sander, U.; D'Arcy, A.; Stihle, M.; Müller, K.; Diederich, D. *Angew. Chem., Int. Ed.* **2003**, *42*, 2507.
10. Paulini, R.; Müller, K.; Diederich, F. *Angew. Chem., Int. Ed.* **2005**, *44*, 1788.
11. Heiden, W.; Goetze, T.; Brickmann, J. *J. Comput. Chem.* **1993**, *14*, 246.
12. Log *D* values were computed at pH 7.5 using the program MoKa (Molecular Discovery Ltd, version 1.1.0). Milletti, F.; Storchi, L.; Sforna, G.; Cruciani, G. *J. Chem. Inf. Model* **2010**, *47*, 2172.
13. Filipski, K. J.; Kohrt, J. T.; Casimiro-Garcia, A.; Van Huis, C. A.; Dudley, D. A.; Cody, W. L.; Bigge, C. F.; Desiraju, S.; Sun, S.; Maiti, S. N.; Jaber, M. R.; Edmunds, J. J. *Tetrahedron Lett.* **2006**, *47*, 7677.
14. Robinson, R. P.; Donahue, K. M. *J. Org. Chem.* **1991**, *56*, 4805.
15. Inhibitory activity expressed as inhibition constant IC_{50} toward recombinant human renin was determined using an assay in which the nonendogenous fluorogenic substrate Dabcyl-γ-Abu-Ile-His-Pro-Phe-His-Leu-Val-Ile-His-Thr-EDANS is cleaved at the Leu–Val bond in analogy to angiotensinogen. Human renin at a concentration of 5 nM is incubated with the test compound at various concentrations and the substrate at a concentration of 10 μM (2 h at RT) in 0.05 M Tris buffer (pH 8). The increase in fluorescence due to fluorescence resonance energy transfer at an emission wavelength of 485 nm is recorded in a microplate spectrofluorometer ([7]).
16. McMartin, C.; Bohacek, R. S. *J. Comput. Aided Mol. Des.* **1997**, *11*, 333.
17. Friesner, R. A.; Banks, J. L.; Murphy, R. B.; Halgren, T. A.; Klicic, J. J.; Mainz, D. T.; Repasky, M. P.; Knoll, E. H.; Shelley, M.; Perry, J. K.; Shaw, D. E.; Francis, P.; Shenkin, P. S. *J. Med. Chem.* **2004**, *47*, 1739.
18. Modeling studies were done using Sybyl 7.3–8.0 (Tripos). Energy calculations were based on the MMFF94s force field (Halgren, T. *J. Comp. Chem.* **1999**, *20*, 720.). Protein-ligand complexes were minimized using the quasi-Newton–Raphson procedure. For manual docking, ligands were placed in the binding site and optimized treating all side chains within 4 Å flexible. Automated docking was carried out using QXP ([16]) or Glide ([17]).
19. Tautomer ratios were computed using the Tauthor approach, as implemented in MoKa (Molecular Discovery Ltd, version 1.1.0). Milletti, F.; Storchi, L.; Sforna, G.; Cross, S.; Cruciani, G. *J. Chem. Inf. Model* **2009**, *49*, 68.
20. The renin-complex for **7d** was prepared by soaking using renin apo-crystals crystallized in hanging drops from conditions described by Lim et al. *J. Mol. Biol.* **1989,** *210,* 239. Data were collected at beam-line ID 23-1 of the European Synchrotron Radiation Facility (ESRF) in Grenoble. The data were processed with mosflm (Leslie, A.G.W. **1992**, Joint CCP4 + ESF-EAMCB Newsletter on Protein Crystallography, No. 33, 22–24). The crystal diffracted to 2.1 Å. The space group was P213 with $a = 138.79$. The inhibitor was fitted using Quanta (Accelrys, 1986–2010) and refined using Buster 2.9.7 (Global Phasing 2011). The coordinates were deposited in the Brookhaven Protein Database (PDB: 3SFC).
21. (a) Burley, S. K.; Petsko, G. A. *Science* **1985**, *229*, 23; (b) McGaughey, G. B.; Gagné, M.; Rappé, A. K. *J. Biol. Chem.* **1998**, *273*, 15458.
22. (a) Recombinant human renin is incubated with the inhibitor at various concentrations plus the substrate Dabcyl-γ-Abu-Ile-His-Pro-Phe-His-Leu-Val-Ile-His-Thr-EDANS at 25 μM for 30 min at 37 °C and 30 min at RT in human or mouse (C57BL6) plasma. Fluorescence is recorded at an excitation wavelength of 330 nm and an emission wavelength of 485 nm. IC_{50} values are calculated from inhibition as function of concentration from multiple measurements.; (b) Permeability studies using Caco-2/TC7 cells are performed using 20 μM compound concentration in the apical to basolateral direction with a pH gradient (6.5–7.4) and a BSA gradient (0.5–5%). After 2 h at 37 °C, the apparent permeability value (Papp) is obtained from quantification [$*10^{-7}$ cm/s].; (c) Physico-chemical properties (pKa, log *P*, log *D*) are computed using MoKa ([12]).; Ligand and lipophilic ligand efficiencies are computed according to: (d) Hopkins, A. L.; Groom, C. R.; Alex, A. *Drug Discovery Today* **2004**, *9*, 430; Leeson, P. D.; Springthorpe, B. *Nat. Rev. Drug Disc.* **2007**, *6*, 881.